

Original Article

Non-Invasive Diagnosis of Type II Diabetes Using Iris-Based Machine Learning Models

Alaa Abdulkareem Ahmed¹, Mohammad Tariq Yaseen^{1*}

¹Department of Electrical Engineering, College of Engineering, University of Mosul, Iraq.

*Corresponding Author : mtyaseen@uomosul.edu.iq

Received: 06 March 2025

Revised: 10 May 2025

Accepted: 22 May 2025

Published: 31 May 2025

Abstract - The increasing occurrence of Type II Diabetes Mellitus (T2DM) due to lifestyle changes has required the development of non-invasive diagnostic methods. This study explores the potential of iridology, another diagnostic approach, joined with machine learning (ML) algorithms to detect T2DM based on a precise Region of Interest (ROI) in the right iris. This work introduces two ML-based classification methods. The first method employs multiple ML models with changing K-fold cross-validation (ranging from 2 to 20 folds), achieving a maximum classification accuracy of 78.5% at 5-fold using Support Vector Machine (SVM) and Binary Generalized Linear Model (GLM) Logistic Regression. The second method employs Principal Component Analysis (PCA) to enhance feature selection, improving accuracy to 82.2% by training predictions from two initial classifiers-Coarse Decision Tree (74.8% at 14-fold, PCA variance 97%) and Linear Discriminant Analysis (77.6% at 9-fold, PCA variance 100%)-before refining classification with a Binary GLM Logistic Regression model. The proposed approach offers a promising, non-invasive alternative for early diabetes detection using iris analysis and Artificial Intelligence (AI).

Keywords - Artificial intelligence, Diabetes detection, Iris-based diagnosis, Machine Learning, Non-Invasive.

1. Introduction

Because those with type 2 diabetes in its early stages may not show any obvious symptoms, the risk of developing the disease increases. The severity of the disease's symptoms varies depending on the condition and its duration [1]. Diabetes Mellitus (DM) is a chronic disease that occurs as a result of the inability of the pancreas to secrete insulin normally, which leads to a deficiency in insulin production, impairment in the functioning of its function, or both, which leads to metabolic disorders of proteins and fats. Over time, high blood sugar leads to damage to the tissues and organs of the body [2][1]. To protect against diabetes, it is necessary to conduct periodic tests to measure blood sugar levels. Most blood sugar tests are performed by taking a blood sample using needles or a scalpel to create an incision. This may be uncomfortable or painful for some, and the process sometimes takes time. Therefore, research is ongoing to develop a non-invasive method for diagnosing diabetes based on iridology [3].

According to the anatomy of the eye, the dynamic visual part of the eyeball consists of the iris and pupil [4]. The iris is the colored circular part surrounding the pupil and is usually lighter in color than the pupil [5] (see Figure 1), which illustrates the anatomy of the eye [4]. The iris consists of tissues rich in properties that make it a useful method for diagnosis in pathology. It consists of five layers of different

complex fibrous tissues, which have rich tissue patterns of small holes, slits, threads, and pigment spots. In addition, there are nerve fibers that constitute approximately 70% of the iris. These nerves are directly connected to the human nervous system and brain. The anatomical characteristics of the iris are affected by functional and hormonal changes, as well as the health status of the human body organs and the circulatory system. These changes are reflected in the tissues of the iris [5].

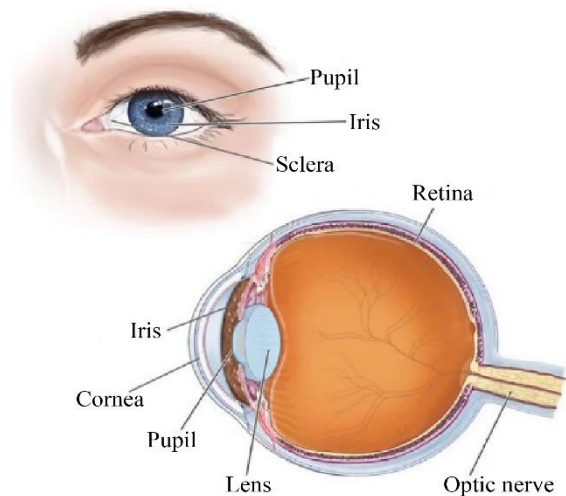


Fig. 1 Human eye anatomy [4]



Therefore, iridology is one of the complementary medical sciences and one of the methods of detecting diseases through the structure of the iris. This is done by observing changes in the pattern, texture, color, and structure of specific areas of each organ in the iris. Weakness and fracture in the tissues of the iris appear long before the symptoms of the disease appear. This reflects the health status of the individual and thus diagnoses problems in the body's organs [5] [6]. Iridologists match their interpretations of diseases with the iris chart. According to Bernard Jensen's classification, the iris chart is divided into a number of regions, about 80 to 90 regions, each representing a different organ of the body [7]. The places of these organs are a reflection of each other in the right and left iris [8], and they are arranged in a shape resembling a clock face [9] (see Figure 2) [10]. As for diabetes, the pancreas region in the modern iris chart is divided into three parts according to the anatomy of the pancreas organ, which consists of the body, tail, and head. In the left iris, the body is located in the region between 7 to 8 o'clock, and the tail between 4 to 5 o'clock. As for the right iris, the head is located between 7 to 8 o'clock. In biomedical applications, advanced image processing and Machine Learning (ML) techniques are widely used in the diagnosis of diseases [7] [6].

This work aims to diagnose type II diabetes using a single ROI in the right iris, representing the head of the pancreas, using ML algorithms for classification. A two-stage classification method consisting of ML algorithms is then used to study the improvement of training accuracy using this method. In this research, the ML method was used in the classification of type II diabetes, with image processing techniques based on the iris chart of the right eye by MATLAB software. Finally, the classification process into diabetes and normal was done using 6 different types of ML algorithms with different k-fold cross-validation and different variance percent of Principal Components Analysis (PCA), and the highest training accuracy was reached at 78.5%. Then, a second approach was proposed to improve the accuracy based on the Validation Confusion Matrix in the trained ML algorithms so that the highest training accuracy obtained was 82.2%.

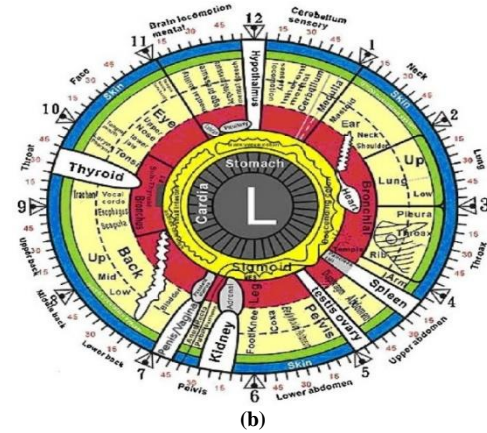


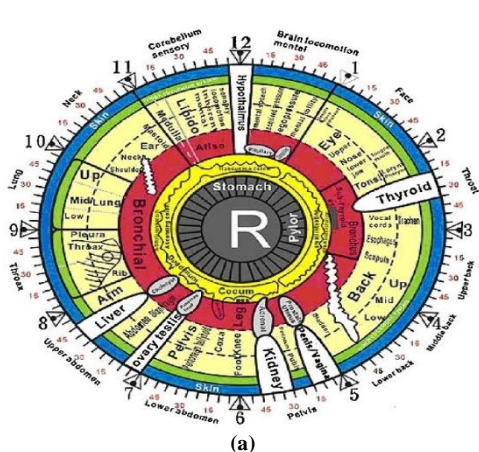
Fig. 2. The iris chart for: (a)Right iris, and (b)Left iris [10]

Also, in this paper, previous work in the field of research will be reviewed, in addition to the materials and research methods, from collecting image datasets to classifying them and predicting the disease, then presenting the results and discussing them, and finally, the conclusions will be reviewed.

2. Related work

Studies on autonomous disease detection using iridology using Artificial Intelligence (AI) algorithms are ongoing. There are many works on diagnosing different diseases with different classification methods. Here, the works related to diagnosing diabetes by iridology are reviewed using different ML classification algorithms. In 2015, A. Bansal et al. [11] proposed an iridology-based system for the diagnosis of type II diabetes. A single Region of Interest (ROI) from the left iris image between 7 and 8 o'clock representing the pancreatic body was used to diagnose diabetes. Features vectors were extracted from this ROI using 2-D discrete wavelet transform (2DWT) by using different combinations of the three sub-band components. The dataset used was 80 eye images of 40 healthy and 40 diabetic individuals; 75% of this dataset was used for training and 25% for testing. In the classification process, the ML algorithm was used for type Support vector machines (SVM) with 4 different kernel functions. The highest accuracy, 87.5%, with 4-fold cross-validation, was obtained using the Radial Basis Function (RBF) kernel function and approximation and horizontal (LL+ HL) sub-bands component features.

Also, in 2015, J. F. Banzi et al. [12] proposed a system that combines computer vision with iridology to examine the patient's iris to predict diabetes in patients using image processing techniques. The ROI for the pancreas was segmented from the right iris image in the region between 01:45 and 02:15 o'clock. The data used was 800 eye images, 400 of which were diabetic and 400 of healthy individuals, which were classified by extracting features from the ROI using adaptive histogram equalization with principal component analysis (PCA) to train the Artificial Neural Network (ANN) type feed-forward backpropagation. When



10 patients, 8 of whom were diabetic, were tested with this system, all of them were diagnosed correctly, indicating that the system's accuracy was 100%. In 2017, R. Agarwal et al. [13] proposed a system that aims to verify iridology in diagnosing diabetes mellitus. The dataset included 200 eye images, 100 of which were diabetic and 100 healthy. The principle of the system, according to the division of the iris chart outline as 60 angles, is based on cropping three ROI from the rectangular rubber sheet normalized, one of them from the right iris between 36'-39' that represents the pancreas's head, and two ROI from the left iris between 38'-41' and 21'-24' that represent pancreas's body and tail respectively. 63 features were extracted and divided into 7 statistical and textures features: Mean Intensity, Standard Deviation, Entropy, Contrast, Correlation, Energy and Homogeneity from ROI directly. In addition, extracted these 7 features were extracted from 3D discrete wavelet transforms (3D-DWT) for each one in eight decompositions. The classification dataset used 6 different ML models. The best accuracy was 89.66% with Random Forest (RF) classifier and 10-fold cross-validation.

Moreover, in 2017, D. C. Adelina et al. [14] proposed a tool to detect pancreatic damage as an indicator of diabetes using iridology. Dataset from 37 eye images were used, 21 of which were normal people and 16 were abnormal people. After preprocessing the images using Gaussian and median filters and then segmenting the image using Circle Hough Transform (CHT), and then normalizing the iris to crop the ROI from the right iris between 7.15-7.45 o'clock. After that, 4 features were extracted by using the Grey Level Co-occurrence Matrix (GLCM) features: Contrast, Energy, Homogeneity, and Entropy. Classification was done using an artificial neural network with a type backpropagation algorithm. When testing 17 images, 6 of which were normal and 11 were abnormal. The accuracy of the system was 82.35%.

Furthermore, in 2018, P. Moradi et al. [15] main goal was to verify iridology for diagnosing diabetes in an automated way using Andreas's regions in the iris. 230 images of people's eyes are used, 106 for diabetic and 124 for healthy. The system works based on preprocessing the images using the active contour algorithm to detect the iris of the rubber sheet model and crop out the ROI. The Gabor filter, the Histogram of Oriented Gradients (HOG), and the Local Binary Pattern (LBP) were used to extract the features-the classification process into normal and abnormal using 5 types of ML algorithms. The work of these researchers is divided into two experiments. The first is to verify the Andreas Cross method with 4 ROI in the form of a cross in each iris representing the regions of diabetes detection, and the results showed the best classification accuracy is 91.8% using the classifier Adaptive Boosting (AdaBoost) at 5-fold and the features pixels, HOG, LBP and Gabor filter. The second experiment aims to identify 4 updated and close regions on Andreas' regions, which will

be used as a new marker for diabetes detection due to the improvement in accuracy over the first experiment by 0.6%, which leads to a better diagnosis. In the same year (2018), P. Samant et al. [6] proposed a system to diagnose type II diabetes using ML by using the total data of 338 subjects (180 diabetic and 158 non-diabetic). The method is based on cropping 3 ROI from the right eye between 7-8 o'clock, which represents the pancreas's head, in the left eye between 7-8 o'clock, which represents the pancreas's body, and between 4-5 o'clock, which represents the pancreas's tail.

Then, extract features from each of this ROI to obtain 180-features divided into 4-first order statistics features and 4-textural GLCM features, as well as 2-d wavelet (DWT) features from ROI for 4 decompositions, for each decomposition and for all possible combinations of these decompositions first order statistics and texture features were computed. These features are selected by feature selection methods to investigate and compute the best suitable feature selection. To classify these features in different classification methods according to depending upon the scoring criterion of each feature selection method, 10 to 50 top-ranked features were selected, with an increment of 10 features. Six different classifiers were used in this research, and performance was evaluated using 10-fold cross-validation. Best classification accuracies have been calculated by the t-test feature selection method as 89.63%, 89.38% for 40 features, and 89.97%, 89.18% for 50 features, by RF and AdaBoost classifiers, respectively.

In 2019, P. Samant et al. [5] introduced a system for diagnosing type II diabetes based on ML, iris-based features, and a combination of physiological parameters. The diagnosis was carried out on 334 samples of iris images, including 250 people with diabetes and 84 healthy people. The system's operation mechanism is the segmentation of the iris using the CHT algorithm. 3 ROI representing the parts of the pancreas was cropped from the iris after the normalization of the rubber sheet, from the right eye between 7-8 o'clock, in the left eye between 7-8 o'clock, and between 4-5 o'clock. 31 features were extracted from each of the three ROIs to determine and detect the condition of tissues in the iris for prediction, and the first features are 5 statistical features. The second features are textural features, including 19 GLCM features. As well as 7 of the Gray-Level Run Length (GLRL) matrix features.

In addition to 20 physiological features, the total number of features is 113. In the classification process, 9 types of supervised ML classifiers are used. The modified t-test with Ensemble Boosted Tree (EBoT) classifier showed the best accuracy of the system of 95.81 %with 10-fold cross-validation. Finally, in 2019, R. Aminah et al. [7] the system proposed a preprocessing of the images from enhancement operations and iris detection by Hough transforms and then normalization using the rubber sheet model. Then, 3 ROI represents the pancreas's head, body, and tail was cropped

from the Right eye between 7-8 o'clock, in the Left eye between 7-8 o'clock, and between 4-5 o'clock. The image dataset was used for 26 people, 16 of whom are non-diabetic and 11 diabetic. The features are extracted from each ROI using GLCM features, namely Contrast, Correlation, Energy, and Homogeneity with different angle orientations ($0^\circ, 45^\circ, 90^\circ, 135^\circ$). Five types of machine learning were used

with 10-fold cross-validation. The best accuracy was 85.6% with k Nearest Neighbor (KNN) type with a specificity of 0.90 and a sensitivity of 0.80. To compare the methodology of previous related works with the current work in terms of the ROI used and the method of adding a second stage of ML algorithms to the classification process, Table 1 is included to show these differences between the works.

Table 1. Comparison of the work methodology between previous works and current work

Reference and Year	ROI in Right Iris (7-8 o'clock)	ROI in Left Iris (4-5 o'clock)	ROI in Left Iris (7-8 o'clock)	Sum of the three ROI in both irises	Four Cross of Andreas Regions	Features Number and Types	k-fold	1- stage or 2-stage ML classification
2015 [11]			✓			180 DWT	4	1
2017 [13]				✓		63 GLCM DWT	10	1
2017 [14]			✓			4 GLCM	-	1
2018 [15]					✓	Gabor LBP HOG	5	1
2018 [6]				✓		180 Statistical GLCMDWT	10	1
2019 [5]				✓		113 Statistical GLCM DWT physiologic	10	1
2019 [7]				✓		GLCM	10	1
This work	✓					10 Entropy GLCM DWT	2 to 20	2

3. Materials and Methods

The proposed stages in building a type II diabetes detection system using ML include a number of basic stages and steps for building any disease detection system using iridology. These basic steps are summarized in collecting the dataset, preprocessing the eye images, finding the ROI for the pancreas, extracting features, and then classifying the dataset to predict the diagnosis, as shown in the diagram in Figure 3.

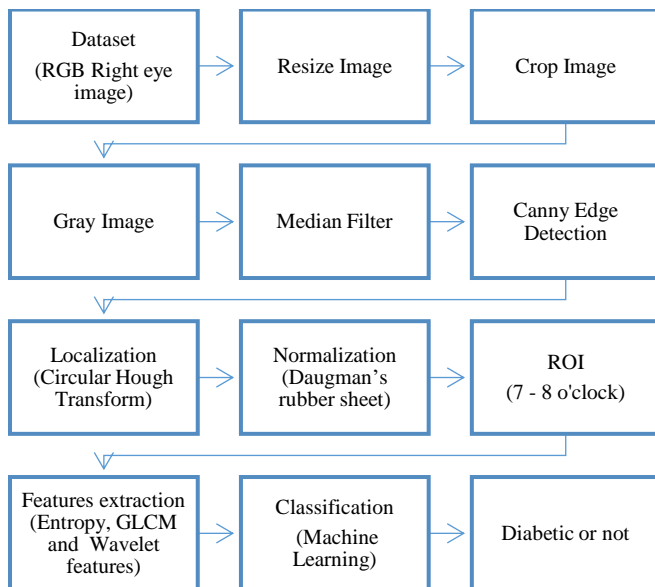


Fig. 3 Block diagram of proposed methodology

All operations system building is done using MATLAB version R2024a.

3.1. Dataset

The first stage in building a diagnostic system is to obtain dataset eye images. The dataset was collected from a previous Research in reference number [15 and is available for free on the GitHub website [16]. The dataset used is 107 images of the right eye.

3.2. Preprocessing

The first stage after obtaining eye images is Preprocessing. It includes a number of operations (see Figure 4), the main purpose of which is to prepare the images for iris detection.

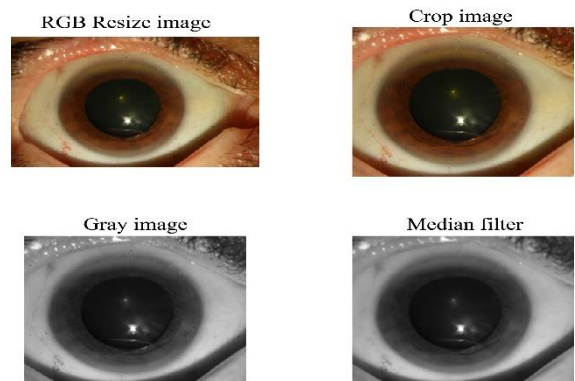


Fig. 4 Preprocessing operation

These operations include first resizing the size of the image to increase the speed of iris localization and, thus, the speed of diagnosis [17]. The second step is cropping the image to remove unimportant areas. The next step is converting the colored image from RGB to grayscale to simplify the processing operations [7]. Then, the median filter was used to smooth and remove noise from the eye images. [18]. For removing outliers without compromising image sharpness, the median filter is superior [19].

3.3. Iris Localization

After the image preprocessing stage, the iris and pupil localization stage begins. Iris localization is typically used to determine the inner and outer boundaries of the iris [10]. This process requires edge detection using the canny technique and iris and pupil detection using the Circular Hough Transform (CHT).

3.3.1. Canny Edge Detection

It is a method used to detect edges of shapes in the image [20]. In this proposed work, the canny edge is used to extract edges from the image with the threshold (0.05) and sigma (3), as shown on the Left side of Figure 5.

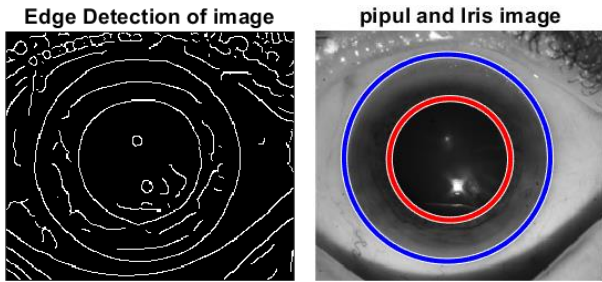


Fig. 5 Left side: canny edge, Right side: localization of iris and pupil

3.3.2. Circular Hough Transform (CHT)

It is a standard computer vision algorithm used to determine the geometric parameters of a circle present in an image [9]. This method is used due to its durability in the presence of noise, clogging, and uneven lighting [21]. The main idea of the Hough transformation is that the points of the Normal plane lie on a circle, and in the Hough plane, there is a corresponding circle; all these circles have one common intersection point (see Figure 6); that is, the transformation of a point in the (x, y) Normal plane to the Hough plane parameter is by Hough transform. A maximum point in the Hough space will correspond to the radius and center coordinates of the circle best defined by the edge points. The circle is expressed, and the directions are Equations below [9].

$$(x - a)^2 + (y - b)^2 = r^2 \tag{1}$$

$$x = a + r \cos(\theta) \tag{2}$$

$$y = b + r \sin(\theta) \tag{3}$$

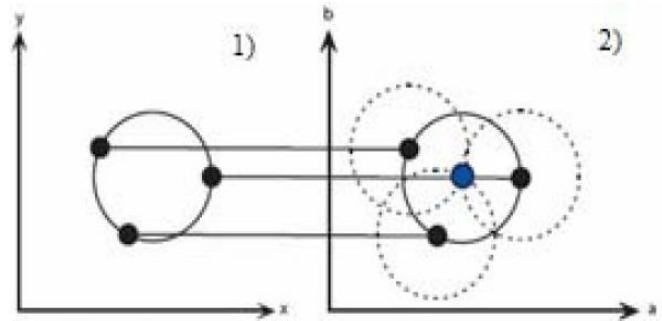


Fig. 6 CHT representation: 1) Normal plane, and 2) Hough plane [9]

Where *a* and *b* are the center coordinates, *r* is the radius, *θ* is the angle, and *x* and *y* are the directions.

In this proposed work, the CHT was used to determine the iris and pupil with a pupil diameter range of [15-70] pixels and an iris diameter range of [78-130] pixels, as shown on the Right side of Figure 5.

3.4. Iris Normalization

After the iris detection stage, the stage of converting it into a rectangular shape begins. Normalization is the process of converting the shape of the iris from polar to rectangular. To make all images of different iris areas the same area and uniform size [14] (see Figure 7) [22], by using Daugman’s Rubber sheet model, the algorithm is based on remaps all points of iris region (x, y) to pair polar coordinates (r, θ), where θ is the angle [0, 2π] and r is on the interval [0,1] [22], the model mapping by equations below [10]:

$$I(x(r, \theta), y(r, \theta)) \rightarrow I(r, \theta) \tag{4}$$

with

$$x(r, \theta) = (1 - r)x_p(\theta) + rx_1(\theta) \tag{5}$$

$$y(r, \theta) = (1 - r)y_p(\theta) + ry_1(\theta) \tag{6}$$

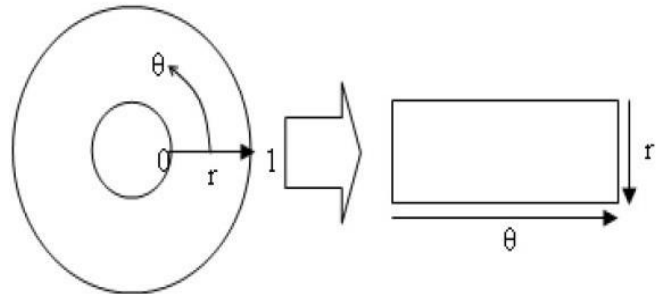


Fig. 7 Daugman’s rubber sheet model [22]

In this work, Daugman’s algorithm was used to convert the iris to a rectangular area with constant dimensions of (361×720) pixels, as shown in the Left side of Figure 8 below.

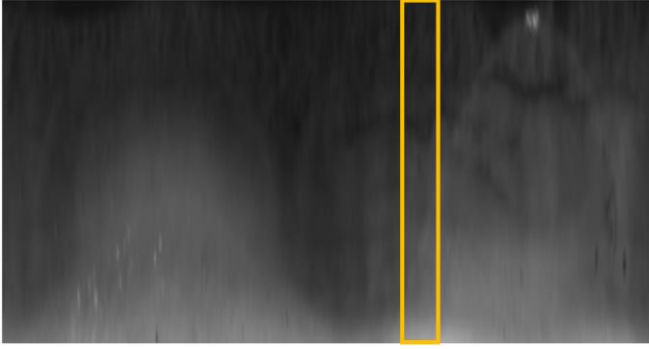


Fig. 8 Right iris normalization and ROI position

3.5. Region of Interest (ROI)

A region of interest (ROI) is a defined region in the iris chart representing the organ to be diagnosed using iridology.

In this work, only one ROI from the right iris between the 7 and 8 o'clock positions, representing the head of the pancreas, was used for diabetes detection. The ROI was cropped from the iris rubber sheet from the previous stage with dimensions of (361×60) pixels (see Figure 8).

3.6. Features Extraction

Feature extraction aims to extract statistical and textural features from the region of interest (ROI) to measure changes in the iris tissue representing the head of the pancreas, manifesting as perforations, tissue fractures, pigmentation, and color changes.

These changes occur as a result of changes in the texture of the ROI tissue as the pancreas changes, reflecting the individual's health status [7]. This research, 10 features were extracted from the ROI by extracting statistical features such as entropy, GLCM, and Wavelet features (see Figure 9).

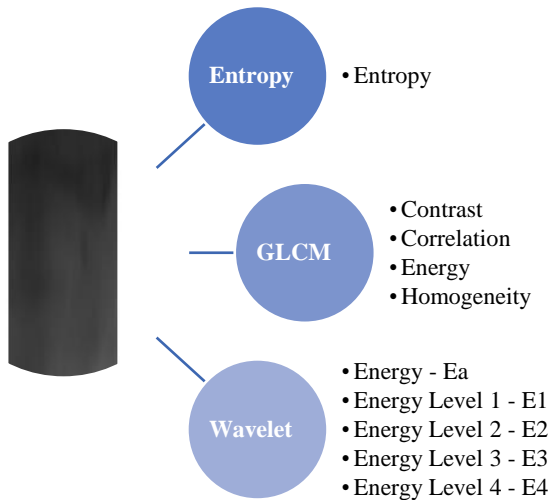


Fig. 9 Ten features from ROI

3.6.1. Entropy Feature

Entropy is a first-order statistical feature that provides information about the gray-level distribution in an ROI [6]. It calculates the complexity of the image texture [5], as in the formula below:

$$Entropy = \sum_{i=1}^{N_1} P(i) \cdot \log_2 P(i) \tag{7}$$

Where P is the first-order histogram with intensity level [6].

3.6.2. GLCM Features

Gray-level co-occurrence Matrix (GLCM) is a second-order statistical method for extracting texture features to calculate the spatial relationship between two pixels.

The GLCM Matrix measures and detects the gray-level intensity of an image by counting the number of repeating pairs of pixels that simultaneously have the same gray level, called the reference pixel and the neighbor pixel [7] [23] [5].

The gray-level intensity is calculated using orientation (θ) and adjacency information represented by the distance between the two pixels (d) (see Figure 10) [24].

The GLCM features extracted from ROI in this work are Contrast, Correlation, Energy, and Homogeneity, with an orientation 0° and pixel distance of 1. Table 2 below shows the formulas and definitions of these features.

Table 2. GLCM features

Features	Definition and Formula [6] [25]
Contrast	Shows the local variations of the image and is calculated as the difference between the highest and lowest values of a continuous group of pixels [5]. $\sum_{i,j} i - j ^2 P(i, j)$
Correlation	measures its gray level linear relationship for image [5]. $\sum_{i,j} \frac{(i - \mu_i)(j - \mu_j)P(i, j)}{\sigma_i \sigma_j}$
Energy	measures an image's texture consistency [5]. $\sum_{i,j} P(i, j)^2$
Homogeneity	It is a local similarity in the image. It measures the closeness of the distribution of elements in the GLCM to the GLCM diagonal [25]. $\sum_{i,j} \frac{P(i, j)}{1 + i - j }$

Where $i = \text{row}$, $j = \text{column}$, and $P = \text{number of pixels}$ [25].

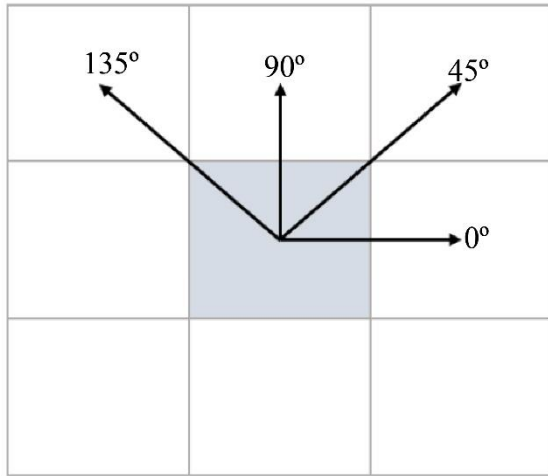


Fig. 10 Direction information for neighbor pixel analysis [24]

3.6.3. Wavelet Features

Discrete Wavelet transform (DWT) is used in medical applications to extract wavelet-based texture features from images [26]. It is a linear process and has the ability to localize the time-space of the spectral features of the signal, unlike the Fourier method [10]. Its utility is to perform the extraction of important features from the iris image [11]; this is done by passing the image signal through two filters, one of which is a low-pass filter and the other a high-pass filter, then the signal is divided into two bands at each filter. The low-pass filter extracts the approximate coefficients from the image, while the high-pass filter extracts the detailed coefficients from the image [26]. Where it analyzes the original iris image of size $N \times N$ into 4 subsamples of images each of size $\frac{N}{2} \times \frac{N}{2}$ which are approximation (LL), horizontal (HL), vertical (LH), and diagonal (HH) [11] (see Figure 11).

In this work used DWT for ROI (see Figure 12) to extract energy from each level of DWT in the Horizontal, Vertical, and Diagonal coefficients (E1, E2, E3, and E4) as well as energy from the Approximation coefficient (Ea), by using fourth level and sym-4 wavelet filter.

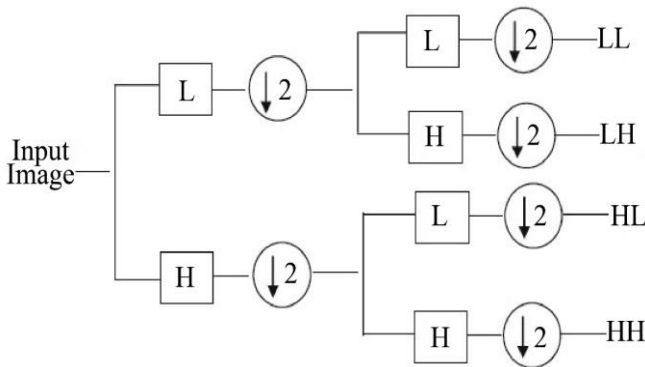


Fig. 11 Single-level DWT analysis of an image [11]

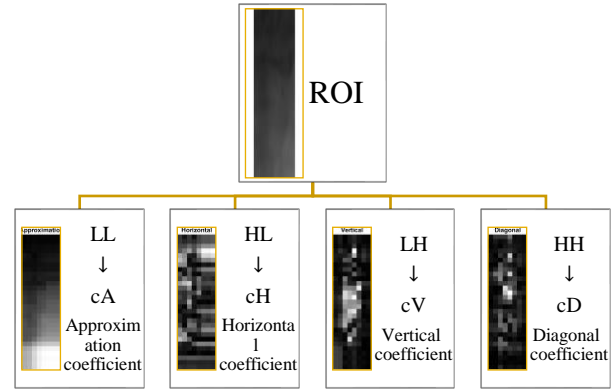


Fig. 12 Wavelet coefficients- one level form ROI

3.7. Classification

True prediction of the 10 features extracted in the previous stage, the label “0” for normal and “1” for diabetic, will be used to train the classifiers on them in this classification stage. The proposed classification method in this work is ML algorithms to identify images of people with diabetes or normal. Moreover, using different K-folds to get the best accuracy. The algorithms were trained using 107 images, 50 of which were of diabetes patients type II and 57 of normal people. The following is an explanation of the tools used in the classification:

3.7.1. Machine Learning (ML)

Machine learning (ML) is a mathematical representation of a real-world scenario. It is a branch of AI that can be used in classification or prediction and is applied in many areas, including healthcare applications. ML model is trained by giving it a set of data called a training dataset, and it is tested on an unseen data set called a test or validation dataset [27]. In this work, 6 ML algorithms are used, and they are: SVM-Linear SVM, Binary GLM Logistic Regression, Tree-Coarse Tree, Linear Discriminant, Ensemble-Bagged Trees, and Ensemble-Subspace Discriminant.

3.7.2. K-Fold Cross Validation

It is an iterative process in which the entire dataset is evaluated and commonly used to evaluate ML models. The dataset is divided into k-folds, with only one k-fold used for testing, while the remaining k-folds are used for training.

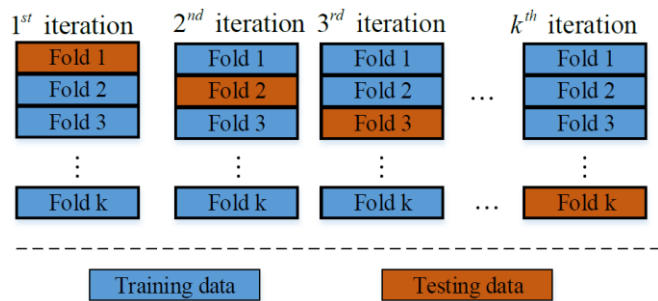


Fig. 13 K-Fold cross validation [27]

This process is repeated in each iteration for each fold (see Figure 13) [27]. In this proposed work, a range of fold values from 2 to 20 folds was used for all 6 ML algorithm models used in classification to determine the best k-fold value for the best classification accuracy.

3.7.3. Principal Component Analysis (PCA)

It is a famous statistical tool that converts a set of highly correlated variables into non-linearly correlated variables using orthogonal transformation [5]. Also, it is a dimensionality reduction technique [28] used to retrieve the most important features found in the data frame [29].

3.7.4. Confusion Matrix

The benefit of the confusion matrix is to find a number of evaluation values for systems such as accuracy as in Equation (8), sensitivity, Specificity, and misclassification error through a number of parameters, which are True Positive (TP), False Positive (FP), True Negative (TN), and False Negative (FN) parameters [3], that can be observed to evaluate the diabetes detection system according to the Table 3, and the Figure 14, that shows the number of images that were misdiagnosed, whether diabetes or normal.

$$Accuracy = \frac{TP+TN}{TP+FP+TN+FN} \times 100\% \tag{8}$$

Table 3. Confusion matrix parameters

Parameter	Meaning
True Positive (TP)	Number of Diabetes iris images that are predicted correctly as diabetes. (Label "1" → label "1")
False Positive (FP)	Number of Normal iris images that are predicted incorrectly as diabetes. (Label "0" → label "1")
True Negative (TN)	Number of Normal iris images that are predicted correctly as Normal. (Label "0" → label "0")
False Negative (FN)	Number of Diabetes iris images that are predicted incorrectly as Normal. (Label "1" → label "0")

Actual Or True	Normal, Label "0"	TN	FP
	Diabetes, Label "1"	FN	TP
Confusion Matrix		Normal, Label "0"	Diabetes, Label "1"
		Predict	

Fig. 14 Confusion matrix details

The proposed work is based on two approaches. Using a single ML algorithm, the first approach was selected based on the highest accuracy of 78.5% at 5-fold, as in Figure 15. The second approach, using three different algorithms in two stages, aims to improve the accuracy of the first approach on the same dataset.

The proposed approach was based on the outputs of the first approach using a PCA process with a variance ranging from 97% to 100%. The highest accuracy of 77.6% was achieved at 9-fold, 15-fold, and 19-fold when PCA variance is 100% by observing the confusion matrix of the ML algorithms that give the highest accuracy at each K-fold when using PCA. The algorithms with the least number of images that were incorrectly diagnosed with false positives (FP) when detecting diabetes and again for images that were incorrectly diagnosed with false negatives (FN) according to the normal condition were determined, and the Tree-Coarse Tree algorithm at 14-fold and PCA variance 97% with least number FP are 2.

The Linear Discriminant algorithm at 9-fold and PCA variance 100% with the least number of FN are 9 were obtained. Based on these two algorithms, the classification was built with these two algorithms. The prediction output for these two algorithms was trained again with the ML algorithm to make the final diagnosis, as shown in Figure 16, so the highest accuracy obtained was 82.2% in many algorithms. The Binary GLM Logistic Regression algorithm has been chosen at 5-fold cross-validation according to the lowest training time, as explained in the Results and Discussion section.

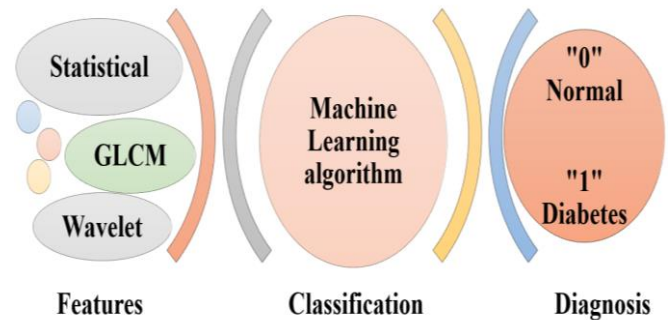


Fig. 15 First proposed approach of classification method

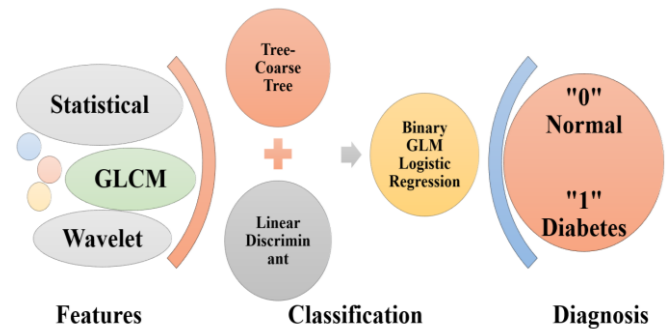


Fig. 16 Second proposed approach of classification method

4. Results and Discussion

In this section, the training classification accuracy results were reviewed using MATLAB for the 6 algorithms and at each K-fold (2-20). For the first proposed approach, Table 4 of ML algorithm training results noted that the algorithms Binary GLM Logistic Regression and SVM-Linear SVM achieved the highest accuracy of 78.5% at 5-fold. Also, the algorithm Binary GLM Logistic Regression achieved the highest accuracy at each fold. So, it is considered the best among the six algorithms, followed by the SVM-Linear SVM algorithm.

Table 4. Results of first proposed approach classification ML algorithms accuracy with K-fold using 10 features

K-fold	Accuracy of Classification of ML Algorithms					
	SVM-Linear SVM	Binary GLM Logistic Regression	Tree - Coarse Tree	Linear Discriminant	Ensemble - Bagged Trees	Ensemble-Subspace Discriminant
	%	%	%	%	%	%
2	67.3	75.7	58.9	70.1	64.5	66.4
3	75.9	74.1	71.4	73.2	68.8	75
4	73.2	77.7	67	74.1	65.2	74.1
5	78.5	78.5	68.2	77.6	74.2	76.6
6	74.8	76.6	64.5	75.7	70.1	73.8
7	75.7	77.6	71	74.8	71	72.9
8	77.6	75.7	72	75.7	67.3	74.8
9	73.8	73.8	69.2	74.8	69.2	74.8
10	77.6	74.8	68.2	74.8	64.5	75.7
11	74.8	77.6	67.3	72	70.1	73.8
12	73.8	75.7	66.4	75.7	68.2	73.8
13	76.6	76.6	72	74.8	70.1	74.8
14	70.1	75.7	65.4	72	70.1	70.1
15	75.7	76.6	68.2	74.8	71	73.8
16	75.7	77.6	70.1	73.8	70.1	75.7
17	72.9	75.7	69.2	72.9	70.1	72.9
18	73.8	76.6	71	75.7	65.4	75.7
19	72.9	74.8	69.2	75.7	68.2	75.7
20	74.8	77.6	72	73.8	69.2	74.8

The second proposed approach idea for the process of improving accuracy is about 78.5% for the same algorithms used and the highest accuracy for these algorithms with different variance PCA. Table 5 noted a PCA variance of 97%; the important features are 2. The Tree algorithms have the highest accuracy, and the least number of normal iris images predicted incorrectly as diabetes (FP) is 2 in Tree-Coarse Tree with the highest accuracy of 74.8% at 14-fold (see Figure 17). While the highest accuracy, 74.8% of the algorithm Ensemble-Bagged Trees at 11-fold, does not give the least number of FP

or the least Number of diabetes iris images that are mispredicted as Normal, whether for detecting diabetes or normal (FN) (see Figure18).

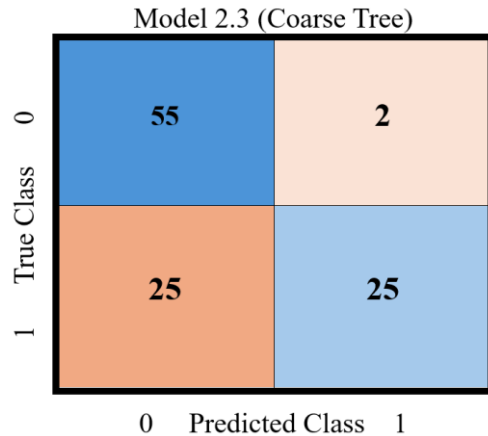


Fig. 17 Confusion matrix – for tree - coarse tree with highest accuracy 74.8%, 14-fold, PCA variance 97%

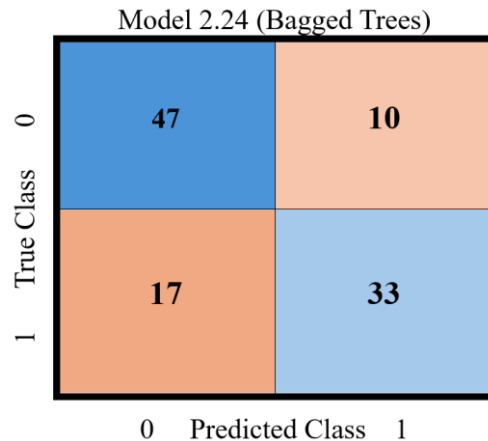


Fig. 18 Confusion matrix – for ensemble – bagged trees with highest accuracy 74.8%, 11-fold, PCA variance 97%

Table 5. Results of classification ML algorithms accuracy with K-fold using PCA variance 97% (2/10 Features)

K-fold	Accuracy of Classification of ML Algorithms					
	SVM-Linear SVM	Binary GLM Logistic Regression	Tree - Coarse Tree	Linear Discriminant	Ensemble - Bagged Trees	Ensemble-Subspace Discriminant
	%	%	%	%	%	%
2	57	61.7	67.3	57	72	62.6
3	61.7	61.7	67.3	61.7	60.7	66.4
4	61.7	64.5	61.7	65.4	65.4	67.3
5	57	58.9	57	60.7	63.6	62.6
6	57.9	59.8	59.8	60.7	59.8	64.5

7	66.4	67.3	70.1	63.6	60.7	67.3
8	66.4	65.4	69.2	65.4	68.2	62.6
9	58.9	64.5	64.5	62.6	63.6	64.5
10	61.7	64.5	63.6	65.4	65.4	64.5
11	62.6	62.6	71	62.6	74.8	65.4
12	60.7	64.5	71	62.6	71	64.5
13	62.6	64.5	72	64.5	62.6	64.5
14	60.7	61.7	74.8	61.7	65.4	61.7
15	59.8	63.6	72.9	60.7	65.4	66.4
16	57.9	63.6	72	61.7	65.4	65.4
17	61.7	63.6	67.3	62.6	59.8	63.6
18	58.9	63.6	69.2	64.5	65.4	61.7
19	63.6	63.6	72	64.5	62.6	64.5
20	58.9	63.6	72.9	61.7	63.6	64.5

7	61.7	64.5	71	63.6	62.6	65.4
8	60.7	61.7	71.1	63.6	63.6	65.4
9	59.8	63.6	62.6	63.6	55.1	63.6
10	62.6	64.5	66.4	62.6	67.3	65.4
11	60.7	63.6	71	61.7	62.6	67.3
12	61.7	62.6	68.2	64.5	65.4	63.6
13	58.9	62.6	73.8	61.7	61.7	60.7
14	61.7	63.6	71	63.6	65.4	60.7
15	61.7	62.6	72	62.6	65.4	64.5
16	63.6	63.6	70.1	62.6	68.2	67.3
17	62.6	65.4	73.8	64.5	69.2	64.5
18	57	62.6	72	61.7	64.5	64.5
19	61.7	65.4	71	62.6	69.2	63.6
20	62.6	63.6	71	64.5	67.3	65.4

When the PCA variance increases to 98%, the important features are 2 features. In the accuracy results in Table 6, it is noted that the Tree algorithm has the highest accuracy in each k-fold and also has the least number of FP are 3 images in Tree-Coarse Tree with the highest accuracy 73.8% at 13-fold and 17-fold (see Figure 19).

When the PCA variance increases to 99%, the important features are 3 features. In the accuracy results in Table 7, it is noted that the Tree algorithm also has the highest accuracy and the least number of FPs, which are 3 images in Tree-Coarse Tree with the highest accuracy at 74.8% at 14-fold (see Figure 20).

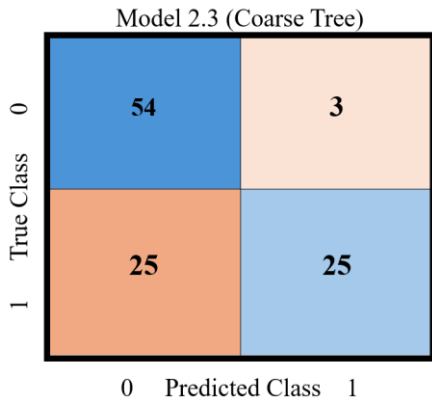


Fig. 19. Confusion matrix – for tree - coarse tree with the highest accuracy 73.8% at 13-fold and 17-fold, PCA variance 98%

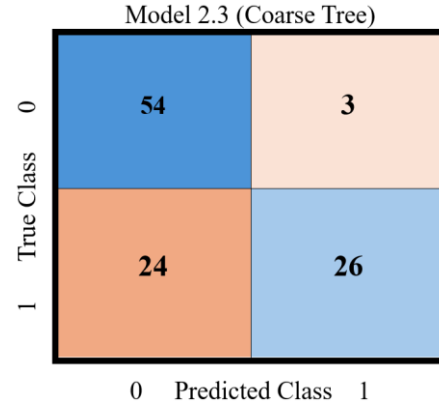


Fig. 20 Confusion matrix – for tree - coarse tree with highest accuracy 74.8%, 14-fold -PCA variance 99%

Table 6. Results of classification ML algorithms accuracy with K-fold using PCA 98% (2/10 Features)

K-fold	Accuracy of Classification of ML Algorithms					
	SVM-Linear SVM	Binary GLM Logistic Regression	Tree - Coarse Tree	Linear Discriminant	Ensemble-Bagged Trees	Ensemble-Subspace Discriminant
	%	%	%	%	%	%
2	57	58.9	58.9	58.9	54.2	60.7
3	62.6	63.6	60.7	63.6	62.6	61.7
4	61.7	64.5	61.7	65.4	67.3	67.3
5	59.8	60.7	65.4	63.6	61.7	67.3
6	62.6	64.5	66.4	62.6	65.4	65.4

Table 7. Results of classification ML algorithms accuracy with K-fold using PCA variance 99% (3/10 Features)

K-fold	Accuracy of Classification of ML Algorithms					
	SVM-Linear SVM	Binary GLM Logistic Regression	Tree - Coarse Tree	Linear Discriminant	Ensemble - Bagged Trees	Ensemble-Subspace Discriminant
	%	%	%	%	%	%
2	56.1	57.9	59.8	57	57.9	65.4
3	60.7	62.6	65.4	66.4	65.4	64.5
4	62.6	62.6	67.3	62.6	61.7	67.3
5	57.9	58.9	63.6	61.7	63.6	59.8
6	61.7	65.4	68.2	66.4	67.3	63.6

7	65.4	62.6	67.3	63.6	65.4	64.5
8	57.9	64.5	70.1	62.6	68.2	63.6
9	62.6	63.6	62.6	60.7	63.6	61.7
10	61.7	63.6	66.4	64.5	64.5	65.4
11	58.9	63.6	71	60.7	64.5	62.6
12	64.5	63.6	68.2	60.7	66.4	62.6
13	60.7	61.7	74.8	59.8	69.2	62.6
14	57.9	62.6	74.8	59.8	65.4	61.7
15	60.7	63.6	72.9	65.4	66.4	65.4
16	63.6	63.6	71	60.7	61.7	64.5
17	61.7	62.6	76.6	63.6	63.6	65.4
18	59.8	61.7	73.8	61.7	59.8	62.6
19	64.5	64.5	69.2	62.6	60.7	64.5
20	63.6	62.6	70.1	61.7	60.7	62.6

6	74.8	75.7	64.8	76.6	70.1	74.8
7	72.9	71	71	72.9	74.8	74.8
8	73.8	73.8	63.6	72	70.1	70.1
9	73.8	76.6	74.8	77.6	76.6	76.6
10	71	75.7	66.4	74.8	70.1	75.7
11	75.7	74.8	63.6	75.7	73.8	75.7
12	72	73.8	70.1	72.9	68.2	72.9
13	72	73.8	72.9	73.8	70.1	72.9
14	72.9	74.8	68.2	72	74.8	72.9
15	75.7	76.6	67.3	74.8	70.1	77.6
16	71	73.8	68.2	72	70.1	72
17	74.8	75.7	66.4	75.7	72.9	75.7
18	72.9	74.8	64.5	73.8	72.9	73.8
19	72	74.8	69.2	74.8	69.2	77.6
20	72.9	74.8	65.4	73.8	67.3	72

When the PCA variance increases to 100%, the important features are 9. The accuracy results in Table 8 noted that the highest classification accuracy is 77.6%, obtained from three algorithms: Linear Discriminant at 9-fold, Ensemble-Subspace Discriminant at 15-fold, and Ensemble-Subspace Discriminant at 19-fold. The first algorithm of these three algorithms gives the least number of FN in 9 images (see Figure 21).

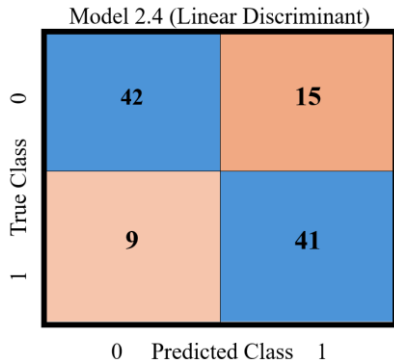


Fig. 21. Confusion matrix – for linear discriminant with the highest accuracy 77.6%, 9-fold -PCA variance 100%

Table 8. Results of classification ML algorithms accuracy with K-fold using PCA variance 100% (9/10 Features)

K-fold	Accuracy of Classification of ML Algorithms					
	SVM-Linear SVM	Binary GLM Logistic Regression	Tree - Coarse Tree	Linear Discriminant	Ensemble - Bagged Trees	Ensemble-Subspace Discriminant
	%	%	%	%	%	%
2	73.8	72.9	69.2	72.9	73.8	72
3	76.6	73.8	67.3	74.8	71	73.8
4	74.8	74.8	68.2	75.7	73.8	76.6
5	72.9	72.9	68.2	72.9	71	74.8

After selecting the output of the two algorithms, Tree-Coarse Tree and Linear Discriminant to train other algorithms to predict more accurately. A number of algorithms were trained with the range of cross-validation from 2 to 10 folds, where the highest accuracy reached was 82.2% for many algorithms.

Algorithm Binary GLM Logistic Regression at 5-fold was chosen according to the shortest training time (0.66387 sec) to be the third algorithm for the second approach in this work, as shown in Table 9. Using two-stage classification in the second proposed approach improves classification accuracy at training by separating the feature data in the first stage using two ML classification algorithms. The classification results in this stage are then separated again using another ML classification algorithm in the second stage.

Table 9. Training times of the ML classification algorithms with the highest training accuracy 82.2% and K-fold used in the third algorithm of the second proposed approach

K-fold	Training Time (sec.)					
	Linear Discriminant	Quadratic Discriminant	Binary GLM Logistic Regression	Naïve Bayes - Gaussian	SVM - Fine Gaussian	SVM - Medium Gaussian
2	-	20.59	-	-	-	-
3	0.96	-	-	2.025	1.281	1.378
4	-	1.755	1.186	1.200	2.024	0.937
5	-	1.7	0.663	0.816	1.209	0.822
6	-	-	-	1.082	0.687	0.946
7	-	0.907	1.786	0.777	2.041	1.026
8	-	3.278	3.484	2.378	0.902	1.654
9	-	0.994	-	1.001	0.898	0.689
10	-	0.980	-	0.813	1.029	0.895

5. Conclusion

This work exhibits the feasibility of detecting Type II Diabetes Mellitus using iris-based machine learning classification models, offering a non-invasive diagnostic alternative to traditional blood tests.

By using advanced image processing techniques and several ML algorithms, this work achieved a classification accuracy of 78.5% in a single-stage approach, which was further enhanced to 82.2% through a two-stage classification model incorporating PCA-based feature selection. The results suggest that iris analysis, combined with ML, has significant potential for diabetes diagnosis with minimal patient discomfort. Future work should focus on expanding dataset

diversity and increasing the number of features extracted from the ROI by extracting different types of features. Additionally, it is proposed that a number of other ML algorithms be added in the first stage of the proposed second approach to improve classification accuracy and robustness.

Funding Statement

This work was conducted without any financial support.

Acknowledgments

The work was supported by the Department of Electrical Engineering, College of Engineering, University of Mosul, Mosul, Iraq. The authors express special gratitude to all of them.

References

- [1] Jai Kumar et al., "A Comparative Analysis of Clinical Features of Diabetes Mellitus Type 2 With Respect to Duration of Diabetes," *Cureus*, vol. 16, no. 11, 2024. [[CrossRef](#)] [[Google Scholar](#)] [[Publisher Link](#)]
- [2] Wantang Li, "Risk Factors and the Treatment of Type 2 Diabetes (T2D)," *Proceedings of the 3rd International Conference on Modern Medicine and Global Health*, vol. 68, no. 1, pp. 115-120, 2025. [[CrossRef](#)] [[Publisher Link](#)]
- [3] Dyla Velia, and Adhi Harmoko Saputro, "Retracted: Designing Diabetes Mellitus Detection System Based on Iridology with Convolutional Neural Network Modeling," *2020 4th International Conference on Informatics and Computational Sciences (ICICoS)*, Semarang, Indonesia, pp. 1-6, 2020. [[CrossRef](#)] [[Google Scholar](#)] [[Publisher Link](#)]
- [4] Marcello Gallerani et al., "Integrated Design and Prototyping of a Robotic Eye System for Ocular and Craniofacial Trauma Simulators," *International Journal on Interactive Design and Manufacturing (IJIDeM)*, vol. 17, no. 6, pp. 3103-3116, 2023. [[CrossRef](#)] [[Google Scholar](#)] [[Publisher Link](#)]
- [5] Piyush Samant, and Ravinder Agarwal, "Analysis of Computational Techniques for Diabetes Diagnosis using the Combination of Iris-Based Features and Physiological Parameters," *Neural Computing and Applications*, vol. 31, no. 12, pp. 8441-8453, 2019. [[CrossRef](#)] [[Google Scholar](#)] [[Publisher Link](#)]
- [6] Piyush Samant, and Ravinder Agarwal, "Machine Learning Techniques for Medical Diagnosis of Diabetes using Iris Images," *Computer Methods and Programs in Biomedicine*, vol. 157, pp. 121-128, 2018. [[CrossRef](#)] [[Google Scholar](#)] [[Publisher Link](#)]
- [7] Ratna Aminah, and Adhi Harmoko Saputro, "Retracted: Application of Machine Learning Techniques for Diagnosis of Diabetes Based on Iridology," *2019 International Conference on Advanced Computer Science and Information Systems (ICACSIS)*, Bali, Indonesia, pp. 133-138, 2019. [[CrossRef](#)] [[Google Scholar](#)] [[Publisher Link](#)]
- [8] Zuraini Othman, and Anton Satria Prabuwono, "Retracted: Preliminary Study on Iris Recognition System: Tissues of Body Organs in Iridology," *2010 IEEE EMBS Conference on Biomedical Engineering and Sciences (IECBES)*, Kuala Lumpur, Malaysia, pp. 115-119, 2010. [[CrossRef](#)] [[Google Scholar](#)] [[Publisher Link](#)]
- [9] K. Sivasankar et al., "Retracted: FCM Based Iris Image Analysis for Tissue Imbalance Stage Identification," *2012 International Conference on Emerging Trends in Science, Engineering and Technology (INCOSSET)*, Tiruchirappalli, India, pp. 210-215, 2012. [[CrossRef](#)] [[Google Scholar](#)] [[Publisher Link](#)]
- [10] Sherif E. Hussein, Osama A. Hassan, and Malcolm H. Granat, "Assessment of the Potential Iridology for Diagnosing Kidney Disease Using Wavelet Analysis and Neural Networks," *Biomed Signal Process Control*, vol. 8, no. 6, pp. 534-541, 2013. [[CrossRef](#)] [[Google Scholar](#)] [[Publisher Link](#)]
- [11] Atul Bansal, Ravinder Agarwal, and R.K. Sharma, "Determining Diabetes Using Iris Recognition System," *International Journal of Diabetes in Developing Countries*, vol. 35, no. 4, pp. 432-438, 2015. [[CrossRef](#)] [[Google Scholar](#)] [[Publisher Link](#)]
- [12] Jamal Firmat Banzi, and Zhaojun Xue, "An Automated Tool for Non-contact, Real Time Early Detection of Diabetes by Computer Vision," *International Journal of Machine Learning and Computing*, vol. 5, no. 3, pp. 225-229, 2015. [[CrossRef](#)] [[Google Scholar](#)] [[Publisher Link](#)]
- [13] Piyush Samant, and Ravinder Agarwal, "Diagnosis of Diabetes Using Computer Methods: Soft Computing Methods for Diabetes Detection Using Iris," *International Journal of Medical, Health, Biomedical, Bioengineering and Pharmaceutical Engineering*, vol. 11, no. 2, pp. 63-68, 2017. [[CrossRef](#)] [[Google Scholar](#)] [[Publisher Link](#)]
- [14] Dyah Ceni Adelina et al., "Retracted: Identification of Diabetes in Pancreatic Organs using Iridology," *2017 International Electronics Symposium on Knowledge Creation and Intelligent Computing (IES-KCIC)*, Surabaya, Indonesia, pp. 114-119, 2017. [[CrossRef](#)] [[Google Scholar](#)] [[Publisher Link](#)]

- [15] Parsa Moradi et al., "Retracted: Discovering Informative Regions in Iris Images to Predict Diabetes," *2018 25th National and 3rd International Iranian Conference on Biomedical Engineering (ICBME)*, Qom, Iran, pp. 1-6, 2018. [[CrossRef](#)] [[Google Scholar](#)] [[Publisher Link](#)]
- [16] The GitHub Website, 2018. [Online]. Available: <https://github.com/NaghmeNazer/diabetes-iridology?tab=readme-ov-file>
- [17] Sandeep Panwar Jogi, and Bharat Bhushan Sharma, "Retracted: Methodology of Iris Image Analysis for Clinical Diagnosis," *2014 International Conference on Medical Imaging, m-Health and Emerging Communication Systems (MedCom)*, Greater Noida, India, pp. 235-240, 2014. [[CrossRef](#)] [[Google Scholar](#)] [[Publisher Link](#)]
- [18] K. Entin Martiana, "Retracted: Application for Heart Abnormalities Detection through Iris," *2016 International Electronics Symposium (IES)*, Denpasar, Indonesia, pp. 315-322, 2016. [[CrossRef](#)] [[Google Scholar](#)] [[Publisher Link](#)]
- [19] P.A. Reshma, and K.V. Divya, and T.B. Subair, "Detection of Heart Abnormalities and High-Level Cholesterol Through Iris," *Proceedings of the International Conference on ISMAC in Computational Vision and Bio-Engineering 2018 (ISMAC-CVB)*, Palladam, India, vol. 30, pp. 339-346, 2019. [[CrossRef](#)] [[Google Scholar](#)] [[Publisher Link](#)]
- [20] David Habsara Hareva, Samuel Lukas, and Natanael Oktavian Suharta, "Retracted: The Smart Device for Healthcare Service: Iris Diagnosis Application," *2013 Eleventh International Conference on ICT and Knowledge Engineering*, Bangkok, Thailand, pp. 1-6, 2013. [[CrossRef](#)] [[Google Scholar](#)] [[Publisher Link](#)]
- [21] Sare Amerifar, Alireza Tavakoli Targhi, and Mohammad Mahdi Dehshibi, "Retracted: Iris the Picture of Health: Towards Medical Diagnosis of Diseases Based on Iris Pattern," *2015 Tenth International Conference on Digital Information Management (ICDIM)*, Jeju, Korea (South), pp. 120-123, 2015. [[CrossRef](#)] [[Google Scholar](#)] [[Publisher Link](#)]
- [22] R.A. Ramlee, and S. Ranjit, "Retracted: Using Iris Recognition Algorithm, Detecting Cholesterol Presence," *2009 International Conference on Information Management and Engineering*, Kuala Lumpur, Malaysia, pp. 714-717, 2009. [[CrossRef](#)] [[Google Scholar](#)] [[Publisher Link](#)]
- [23] L.B. Rachman, and Basari, "Detection of Cholesterol Levels by Analyzing Iris Patterns using Backpropagation Neural Network," *The 2nd Tarumanagara International Conference on the Applications of Technology and Engineering (TICATE)*, Jakarta, Indonesia, vol. 852, no. 1, pp. 1-8, 2020. [[CrossRef](#)] [[Google Scholar](#)] [[Publisher Link](#)]
- [24] Ferdi Özbilgin, Çetin Kurnaz, and Ertan Aydın, "Prediction of Coronary Artery Disease Using Machine Learning Techniques with Iris Analysis," *Diagnostics*, vol. 13, no. 6, pp. 1-20, 2023. [[CrossRef](#)] [[Google Scholar](#)] [[Publisher Link](#)]
- [25] Melvin Daniel, Jangkung Raharjo, and Koredianto Usman, "Iris-based Image Processing for Cholesterol Level Detection using Gray Level Co-Occurrence Matrix and Support Vector Machine," *Engineering Journal*, vol. 24, no. 5, pp. 135-144, 2020. [[CrossRef](#)] [[Google Scholar](#)] [[Publisher Link](#)]
- [26] Kumar Mohit, Rajeev Gupta, and Basant Kumar, "A Survey on the Machine Learning Techniques for Automated Diagnosis from Ultrasound Images," *Current Medical Imaging Formerly Current Medical Imaging Reviews*, vol. 20, no. 1, pp. 1-15, 2023. [[CrossRef](#)] [[Google Scholar](#)] [[Publisher Link](#)]
- [27] Isaac Kofi Nti, Owusu Nyarko-Boateng, and Justice Aning, "Performance of Machine Learning Algorithms with Different K Values in K-fold CrossValidation," *International Journal of Information Technology and Computer Science*, vol. 13, no. 6, pp. 61-71, 2021. [[CrossRef](#)] [[Google Scholar](#)] [[Publisher Link](#)]
- [28] Carlos Fernandez-Grandon, Ismael Soto, and David Zabala-Blanco, "Extreme Learning Machine for Iris-Based Diabetes Detection," *2023 IEEE CHILEAN Conference on Electrical, Electronics Engineering, Information and Communication Technologies (CHILECON)*, Valdivia, Chile, pp. 1-6, 2023. [[CrossRef](#)] [[Google Scholar](#)] [[Publisher Link](#)]
- [29] C. Yohannes, I. Nurtanio, and K.C. Halim, "Potential of Heart Disease Detection Based on Iridology," *The 3rd EPI International Conference on Science and Engineering 2019 (EICSE2019)*, South Sulawesi, Indonesia, vol. 875, no. 1, pp. 1-9, 2020. [[CrossRef](#)] [[Google Scholar](#)] [[Publisher Link](#)]